Polymer Journal (2014) 46, 250–253

www.nature.com/pj

NOTE

Birefringence behavior of a flexible S-SEB-S/PPE nano-alloy

Yoshifumi Araki[1], Kosuke Nakatani[1], Yukari Hori[1], Katsumi Suzuki[1], Hiroshi Shirai[1], Kiyoo Kato[1] and Hiromu Saito[2]

Polymer Journal (2014) **46,** 250–253; doi:10.1038/pj.2013.94; published online 22 January 2014

Keywords: blend; birefringence; phtoelastic coefficient; polyphenylene ether; thermoplastic styrenic elastomer

INTRODUCTION

Flexible and flame-retardant materials are desired for use in wire-coating materials, including flexible wire insulation, USB cables, cell phone chargers/adapters and internal wiring. Poly(2,6-dimethyl-l,4-phenylene ether) (PPE) is an excellent flame-retardant material,[1,2] but it is brittle and not easily processed. The mechanical properties and processability of PPE have often been improved by blending thermoplastic styrenic elastomers (TPSs), which consist of outer glassy polystyrene (PS) block segments and middle rubbery block segments, such as styrene-*b*-butadiene-*b*-styrene triblock copolymer and its hydrogenated version styrene-*b*-ethylene-*co*-butylene-*b*-styrene triblock copolymer,[3–7] because PPE is solubilized by the PS block segments in TPS.[8,9] However, PPE is usually phase separated from TPS on the micrometer scale when the molecular weight and/or the content of styrene segments of TPS is low,[10,11] and its flame-retardant property is inferior at low PPE compositions. Alternatively, PPE can be solubilized with TPS and exhibits flame-retardant properties at low PPE compositions when the molecular weight and/or content of styrene segments of TPS is high;[11] however, the blend is not flexible. Hence, obtaining flexible and flame-retardant materials remains difficult due to the trade-off between these properties.

Recently, we found that both material flexibility and flame-retardant properties could be achieved by blending TPS with a modified PPE and using a hydrogenated styrene-*b*-styrene-*co*-butadiene-*b*-styrene triblock copolymer (S-SEB-S),[12] though the styrene content of the TPS is high (67 wt%) (Araki *et al.*, submitted). The stress at 100% strain is below 6 MPa and the strain at the break is above 250%, which are similar to those of flexible polyvinyl chloride. To understand the origin of flexibility of the S-SEB-S/modified PPE despite its blending of the high-styrene-content S-SEB-S with high-strength PPE, in this paper, we demonstrate the results of simultaneous stress and birefringence measurements during uniaxial stretching. This method was selected because (1) birefringence is sensitive to changes in orientation with small deformations; (2) the *in situ* measurement of high-speed deformation processes is possible with fast measurements; and (3) the microdomain and matrix segment orientations can be evaluated separately.[13,14] The orientation behavior is discussed with the stress-optical coefficient.

EXPERIMENTAL PROCEDURE

The S-SEB-S (A-B-A type) triblock copolymer was prepared using a two-stage process as described in the previous paper (Araki *et al.*, submitted).[15] The pre-hydrogenated S-SEB-S specimen (S-SB-S) was first synthesized, followed by hydrogenation of the unsaturated butadiene double bonds in S-SB-S. Polymerization of S-SB-S was sequentially performed through anionic polymerization using *n*-butyl lithium as an initiator in a cyclohexane solvent. After the first PS block was polymerized via styrene monomer addition, styrene and butadiene monomers were simultaneously added at a constant rate to generate the SB middle block, and then a styrene monomer was added to polymerize the second PS outer block. S-SB-S hydrogenation was performed using a titanocene catalyst in a cyclohexane solvent. The styrene contents of the two outer PS blocks and the SEB middle block were 20 wt% and 47 wt%, respectively, and the total styrene content in S-SEB-S was 67 wt%. The average molecular weights of the S-SEB-S and PS outer block segments in the S-SEB-S were 99 000 and 9900, respectively.

The modified PPE used in this study is a commercial product (X1010, Asahi Kasei Chemicals Co, Tokyo, Japan) in which PPE (Mn = 18 000) was blended with PS at a PPE composition of 70 wt%.

The S-SEB-S was melt-mixed with the modified PPE using a twin-screw extruder, having a screw diameter of 32 mm (TEX30α, The Japan Steel Works, Ltd, Tokyo, Japan), at a rotation speed of 250 r.p.m. and an operating temperature of 250 °C. Film specimens with thicknesses of 2–0.2 mm were prepared for transmission electron microscopy observations and simultaneous stress and birefringence measurements, respectively, by press molding at 220 °C.

For transmission electron microscopy, ultrathin sections of approximately 70 nm thickness were cut from the film specimen with a cryomicrotome. The sections were stained with ruthenium tetroxide (RuO_4) vapor for 5 min at room temperature. The morphologies were observed using a TEM (JEM 1230, Jeol, Ltd, Tokyo, Japan) with an acceleration voltage of 80 kV.

[1]Asahi Kasei Chemicals Corporation, Kawasaki, Kanagawa, Japan and [2]Department of Organic and Polymer Materials Chemistry, Tokyo University of Agriculture and Technology, Koganei-shi, Tokyo, Japan
Correspondence: Y Araki, Laboratory of Plastics, Asahi Kasei Chemicals Corporation, 1-3-1 Yakoh, Kawasaki-ku, Kawasaki, Kanagawa 210-0863, Japan.
E-mail: araki.yb@om.asahi-kasei.co.jp
Received 22 September 2013; revised 6 November 2013; accepted 23 November 2013; published online 22 January 2014

Stress and birefringence were measured using a specially designed apparatus as previously described.[13,14,16] The specimen was fastened with clamps that were 15 mm apart and stretched at 25 °C at a constant strain rate of 0.3 per second. For birefringence measurements, a He–Ne laser beam with a wavelength (λ_o) of 632.8 nm was passed through a Gran–Thomson prism polarizer, a photoelastic modulator, a film specimen, a Gran–Thomson analyzer and a photodiode detector. The force and the retardation (δ) were measured by the load cell and the photodiode, respectively, and were processed by a personal computer through an A/D converter. The nominal birefringence (Δn_n) is given by $\Delta n_n = \delta \times \lambda_o / 2\pi d$, where d is the thickness of the unstretched film specimen. The nominal stress was obtained after dividing the force by the cross-sectional area of the unstretched film specimen.

RESULTS AND DISCUSSION

Figure 1 shows the transmission electron microscopy micrographs of the S-SEB-S triblock copolymer and the S-SEB-S/modified PPE in the ratio 67/33. A two-phase spherical domain structure with a size of several tens of nanometers can be seen in the S-SEB-S (Figure 1a). Because RuO_4 preferentially stains styrene, the dark spherical domain region can be assigned to the PS outer-block segments. Thus, hard-PS microdomains of several tens of nanometers in diameter are dispersed throughout the continuous soft SEB matrix. Conversely, a two-phase lacy structure is observed in the blend (Figure 1b). This lacy structure consists of domains surrounded by a lacy matrix; the size of the domain and the diameter of the network are approximately 100 and 30 nm, respectively. Thus, a nano-alloy consisting of a two-phase structure on the nanometer scale was obtained. Because RuO_4 also preferentially stains PPE, light matrix regions can be assigned to the soft SEB phase, whereas the dark domain regions can be assigned to the mixed phase of PS and PPE. This lacy pattern occurs due to the solubilization of PPE with PS; the modified PPE is inserted into the PS domains of the S-SEB-S, though the outer PS-block segment content in the S-SEB-S is low (20 wt%). Thus, hard PS/PPE domains are dispersed throughout the continuous soft SEB matrix.

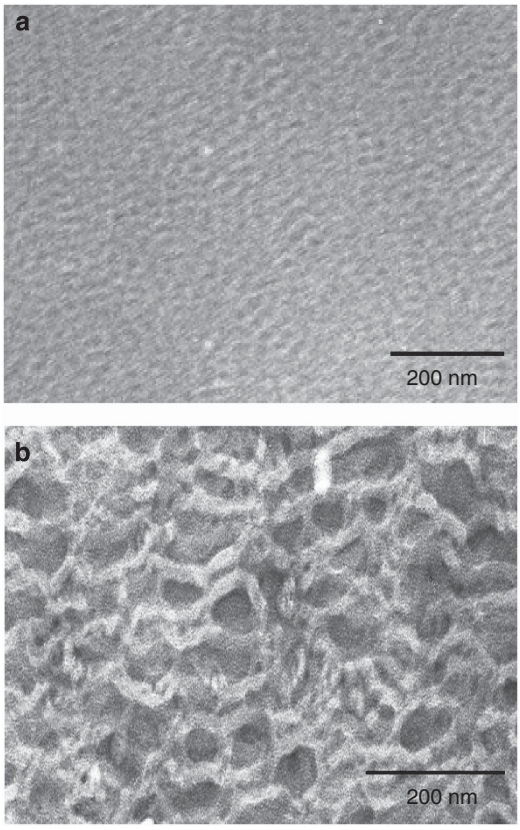

Figure 1 Transmission electron microscopy images of (**a**) S-SEB-S and (**b**) 67/33 S-SEB-S/modified PPE.

Figure 2 shows the stress (σ)–strain (ε) behaviors of the S-SEB-S and the 67/33 S-SEB-S/modified PPE nano-alloy; the structures are demonstrated in Figure 1. By assuming that the contraction rate of thickness and that of width are the same during uniaxial stretching, nominal stress σ_n and nominal birefringence Δn_n were converted into true stress by the formula $\sigma = \sigma_n (W/W_o)^2$ and true birefringence by $\Delta n = \Delta n_n / (W/W_o)$, respectively, where W is the width of the stretched specimen and W_o is the width of the unstretched specimen. The stress increased with an increase in strain. The stress and the modulus estimated from the initial slope were low in the S-SEB-S material. This mechanical behavior is typical of rubbers, even though the total content of the brittle styrene component was high (67 wt%). The stress–strain curve shape of the nano-alloy was similar to that of the S-SEB-S. The yield point was not observed, and the stress at 100% strain was low (<6 MPa). The elastic modulus of the nano-alloy estimated from the initial slope of the stress at strain $<10\%$ was nearly the same as that of the S-SEB-S. These results indicate that the nano-alloy maintains the flexibility of rubber even though high-strength PPE is inserted in the PS domain. As a result of the insertion of the modified PPE in the PS domain of the S-SEB-S, stress of the nano-alloy was larger than that of the S-SEB-S at a strain $>10\%$. This result is due to the high-stress concentration generated near the interphase of the glassy domain and the rubbery matrix during the deformation of the rubbery matrix.

Figure 3 shows the birefringence (Δn)–strain (ε) behavior of the S-SEB-S material and the 67/33 S-SEB-S/modified PPE nano-alloy. Interestingly, the birefringence exhibited a negative value, though it is known that birefringence values of PS and EB segments are positive at 25 °C. The birefringence value of PS changes the sign from positive to negative after heating from the glassy state to the rubbery or melt state, above the glass transition temperature (T_g).[16,17] As the recorded measurement temperature (25 °C) is above the T_g of the SEB matrix (*ca.* 10 °C),[12] the negative birefringence might be attributed to the orientation of the styrene segments in the rubbery SEB matrix due to its large mobility above the T_g in the rubbery SEB matrix. The negative birefringence increased steadily with increasing strain from the initial level in both the S-SEB-S sample and the nano-alloy, and the difference in birefringence values was small. These results suggest that the rubbery SEB matrix is oriented by the initial strain in both the S-SEB-S material and the nano-alloy.

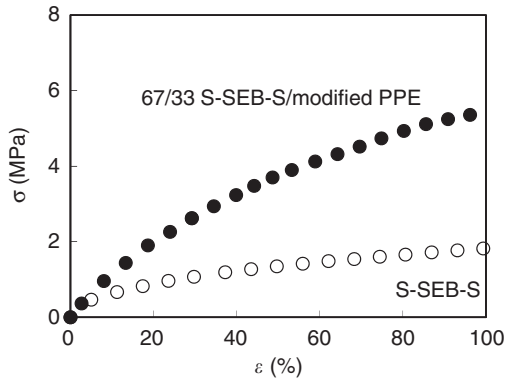

Figure 2 Stress of S-SEB-S and 67/33 S-SEB-S/modified PPE under strain during uniaxial stretching.

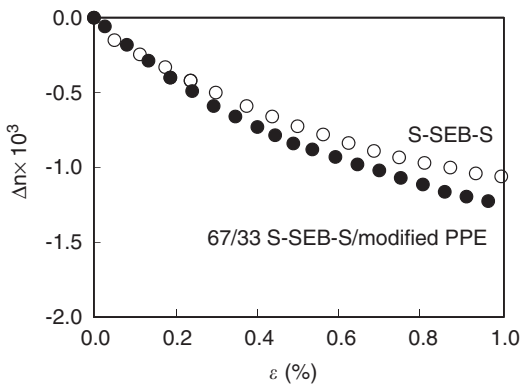

Figure 3 Birefringence of S-SEB-S and 67/33 S-SEB-S/modified PPE under strain during uniaxial stretching.

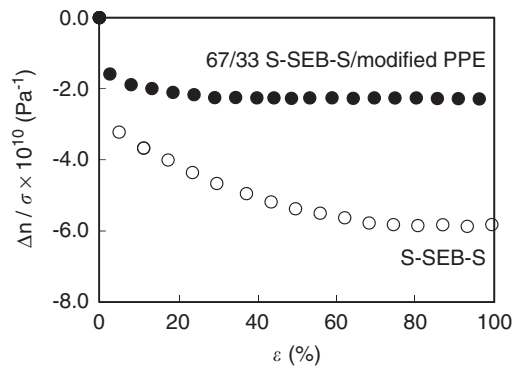

Figure 4 $\Delta n/\sigma$ of S-SEB-S and 67/33 S-SEB-S/modified PPE under strain during uniaxial stretching.

The photoelastic coefficient, $\Delta n/\sigma$, of a rubber segment is given by[18]

$$\frac{\Delta n}{\sigma} = \frac{2\pi}{45kT} \cdot \frac{(\overline{n}^2+2)^2}{\overline{n}} \cdot (b_1 - b_2). \quad (1)$$

The $\Delta n/\sigma$ is expected to be constant with strain when the σ and Δn originate from the orientation of the rubbery segments. The $\Delta n/\sigma$ of the S-SEB-S and the nano-alloy was obtained from σ and Δn as shown in Figures 2 and 3, respectively. The results are shown as a function of strain in Figure 4. The negative $\Delta n/\sigma$ of the S-SEB-S increased at a strain of $<70\%$ and then became constant at a strain of $>70\%$. Note here that the form birefringence, attributed to the anisotropic shape of the PS domains, might contribute to the increase of the photoelastic coefficient,[13,19] but it could not be separated because the birefringence increased continuously with strain. Because the $\Delta n/\sigma$ is constant with strain only when the rubbery segment is oriented, the constant $\Delta n/\sigma$ at a strain $>70\%$ is attributed to the rubbery SEB matrix orientation ($\Delta n = \Delta n_{\mathrm{rSEB}}$). The increase of the $\Delta n/\sigma$ at a strain of $<70\%$ is attributed to the orientation of both the rubbery SEB matrix and the glassy PS domain ($\Delta n = \Delta n_{\mathrm{rSEB}} + \Delta n_{\mathrm{gPS}}$). Thus, the results suggest a two-step orientation of the S-SEB-S: (1) both the rubbery SEB matrix and the glassy PS domains are oriented at a strain of $<70\%$; and (2) only the rubbery SEB matrix is oriented at a strain of $>70\%$. Owing to the two-step orientation, the increase of the stress with strain was large in the low-strain region due to the orientation of both the glassy PS domains and the rubbery SEB matrix, whereas it became smaller in the high-strain region due to the orientation of only the rubbery SEB matrix, as shown in Figure 2.

The $\Delta n/\sigma$ change in the nano-alloy is similar to that in the S-SEB-S sample, indicating that the nano-alloy is also oriented in a two-step process due to its rubbery SEB matrix, as is the case of S-SEB-S shown in Figure 1. The $\Delta n/\sigma$ of the nano-alloy was smaller than that of the S-SEB-S because the σ of the nano-alloy was larger than that of the S-SEB-S, whereas the Δn was approximately the same, as demonstrated in Figures 2 and 3. The $\Delta n/\sigma$ of the nano-alloy became constant at a lower strain compared with that of the S-SEB-S material (that is, the $\Delta n/\sigma$ of the nano-alloy became constant at a strain of $>30\%$, whereas the $\Delta n/\sigma$ of the S-SEB-S became constant at a strain of $>70\%$). These results indicate that only the soft SEB segments are oriented from the lower-strain region in the nano-alloy compared with the S-SEB-S sample, suggesting that the orientation of the glassy PS domain is suppressed by the modified PPE inserted into the PS domain and surrounded by the rubbery SEB matrix. As a result of the rubbery SEB matrix orientation, the tensile property of the nano-alloy is flexible, as is the case of the S-SEB-S sample, even though the high-styrene-content S-SEB-S is blended with a high-strength PPE.

CONCLUSION

Here, we obtained a flexible nano-alloy with a continuous soft, lacy SEB matrix after blending high-styrene-content S-SEB-S with a modified PPE. The simultaneous stress and birefringence measurements revealed that (1) the birefringence exhibits a negative value due to the large mobility of the styrene segments in the SEB matrix; (2) the nano-alloy is oriented in a two-step process, as in the case of the S-SEB-S (that is, both the rubbery SEB matrix and the glassy domains are oriented in the low-strain region, whereas only the rubbery SEB matrix is oriented in the high-strain region); and (3) the orientation of the glassy domain is suppressed, and only the soft SEB segments are oriented from the lower strain region in the nano-alloy when compared with those in the S-SEB-S material. Consequently, the S-SEB-S/PPE nano-alloy is flexible despite its blending of the high-styrene-content S-SEB-S with a high-strength PPE. Details regarding the structure and flame-retardant properties of this material compared with those of various thermoplastic styrenic elastomers are presented in a separate paper (Araki *et al.*, submitted).

1 Boscoletto, A. B., Checchin, M., Milan, L., Pannocchia, P., Tavan, M., Camino, G. & Luda, M. P. Combustion and fire retardance of poly(2,6-dimethyl-1,4-phenylene ether)-high-impact polystyrene blends. *J. Appl. Polym. Sci.* **67,** 2231–2241 (1998).
2 Wang, X., Feng, W., Li, H. & Ruckenstein, E. Optimum toughening via a bicontinuous blending: toughening of PPO with SEBS and SEBS-g-maleic anhydride. *Polymer (Guildf.)* **43,** 37–43 (2002).
3 Mazard, C., Benyahia, L. & Tassin, J. F. Dynamic mechanical properties of polystyrene-based block copolymers blended with poly(2,6-dimethyl-1,4-phenylene oxide). *Polym. Int.* **52,** 514–521 (2003).
4 Tucker, P. S., Barlow, J. W. & Paul, D. R. Molecular weight effects on phase behavior of blends of poly(phenylene oxide) with styrenic triblock copolymers. *Macromolecules* **21,** 2794–2800 (1988).
5 Deanin, R. D. & Lunn, P. Polyblends of Polyphenylene Ether With Styrene-Ethylene/Butylene-Styrene Block Copolymer. *Society of Plastics Engineers Annual Technical Conference* **58,** 2113–2115 (2000).
6 Chiu, H. T. & Hwung, D. S. Miscibility study on polyphenylene oxide and SBS triblock copolymer blends. *Eur. Polym. J.* **30,** 1191–1195 (1994).
7 Puskas, J. E., Kwon, Y., Altstadt, V. & Kontopoulou, M. Blends of poly(2,6-dimethyl-1,4-phenylene oxide)(PPO) with polystyrene-based thermoplastic rubbers: a comparative study. *Polymer (Guildf.)* **48,** 590–579 (2007).
8 Shultz, A. R. & Gendron, B. M. Thermo-optical and differential scanning calorimetric observations of mobility transitions in polystyrene-poly(2,6-dimethyl-1,4-phenylene oxide) blends. *J. Appl. Polym. Sci.* **16,** 461–471 (1972).
9 Machate, C., Lohmar, J. & Droscher, M. Plastic-rubber composite, 1. The polymer-polymer interdiffusion at the phase boundary of poly(oxy-2,6-dimethyl-1,4-phenylene) and polystyrene. *Makromol. Chem.* **191,** 3011–3023 (1990).

10 Izumoto, T., Umeda, H., Sakurai, S., Masamoto, J., Momura, S., Kitagawa, Y. & Suda, Y. Solubility of poly(phenylene ether) to polystyrene-*block*-polyethylenebutylene-*block*-polystyrene triblock copolymers. *SEN' I GAKKAISHI* **55,** 54–61 (1999).
11 Hashimoto, T., Kimishima, K. & Hasegawa, H. Self-assembly and patterns in binary mixtures of SI block copolymer and PPO. *Macromolecules* **24,** 5704–5712 (1991).
12 Araki, Y., Shimizu, D., Hori1, Y., Nakatani, K. & Saito, H. Mechanical properties and microphase structure of hydrogenated S-SB-S triblock copolymers. *Polym. J.* **45,** 1140–1145 (2013).
13 Shimizu, K. & Saito, H. Orientation of cylindrical microdomains of triblock copolymers by in situ stress-strain-birefringence measurements. *J. Polym. Sci. Pt. B Polym. Phys.* **47,** 715–723 (2009).
14 Shimizu, K. & Saito, H. Orientation relaxation of triblock copolymer with cylindrical microdomain by in situ stress-birefringence measurements. *Polym. J.* **41,** 562–567 (2009).
15 Yoshida, J. & Friedrich, C. Thermorheological properties of hydrogenated pseudorandom styrene-butadiene copolymers. *Macromolecules* **38,** 7164–7173 (2005).
16 Takahashi, S. & Saito, H. Conformational change of phenyl ring side group during stress relaxation in glassy poly(styrene-co-acrylonitrile). *Macromolecules* **37,** 1062–1066 (2004).
17 Rudd, J. F. & Andrews, R. D. Photoelastic properties of polystyrene in the glassy state. III. Styrene derivatives and copolymers. *J. Appl. Phys.* **31,** 818 (1960).
18 Treloar, L. R. G. *The Physics of Rubber Elasticity* 174–209 (Oxford University Press, Oxford, 2005).
19 Tamura, E., Kawai, Y., Inoue, T. & Watanabe, H. Rheo-optical study of viscoelastic relaxation modes in block copolymer micellar lattice system. *Macromolecules* **45,** 6580–6586 (2012).